PHYSICAL REVIEW D **90,** 064012 (2014)

Mixing of spherical and spheroidal modes in perturbed Kerr black holes

Emanuele Berti* and Antoine Klein†

Department of Physics and Astronomy, The University of Mississippi, University, Mississippi 38677, USA

(Received 15 August 2014; published 8 September 2014)

The angular dependence of the gravitational radiation emitted in compact binary mergers and gravitational collapse is usually separated using spin-weighted spherical harmonics ${}_sY_{\ell m}$ of spin weight s, that reduce to the ordinary spherical harmonics $Y_{\ell m}$ when $s=0$. Teukolsky first showed that the perturbations of the Kerr black hole that may be produced as a result of these events are separable in terms of a different set of angular functions: the spin-weighted *spheroidal* harmonics ${}_sS_{\ell mn}$, where n denotes the "overtone index" of the corresponding Kerr quasinormal mode frequency $\omega_{\ell mn}$. In this paper we compute the complex-valued scalar products of the ${}_sS_{\ell mn}$'s with the ${}_sY_{\ell m}$'s ("spherical-spheroidal mixing coefficients") and with themselves ("spheroidal-spheroidal mixing coefficients") as functions of the dimensionless Kerr parameter j. Tables of these coefficients and analytical fits of their dependence on j are available online for use in gravitational-wave source modeling and in other applications of black-hole perturbation theory.

DOI: 10.1103/PhysRevD.90.064012 PACS numbers: 04.70.-s, 04.25.dg, 04.30.Db, 04.30.Nk

I. INTRODUCTION

Various angular functions, including scalar, vector, and tensor spherical harmonics, are used to perform separation of variables in the general relativity literature. These functions include the Regge-Wheeler harmonics, the symmetric, trace-free tensors of Sachs and Pirani, the Newman-Penrose spin-weighted spherical harmonics, and the Mathews-Zerilli Clebsch-Gordan-coupled harmonics. An excellent review article by Thorne [1] lists all of these functions and discusses their mutual relations.

The spin-weighted spherical harmonics ${}_sY_{\ell m}$ [2,3] are most commonly used to separate the angular dependence of the gravitational radiation emitted as a result of compact binary mergers and gravitational collapse in numerical relativity simulations. Unfortunately, the ${}_sY_{\ell m}$'s are not ideal to study the perturbations of the rotating Kerr black holes of mass M and dimensionless angular momentum $j \equiv a/M$ that may be formed as a result of compact binary mergers or gravitational collapse (here and below a is the usual Kerr parameter, and we use geometrical units: $G=c=1$).

Teukolsky [4,5] first realized that the radiation produced by perturbed Kerr black holes is most conveniently studied using a different set of angular functions: the spin-weighted spheroidal harmonics ${}_sS_{\ell m}(a\omega)$ (henceforth SWSHs). The differential equation defining these functions is a generalized spheroidal wave equation [6], and it results from separating variables in the partial differential equations describing the propagation of a spin-s field in a rotating (Kerr) black hole background. If we use the Kinnersley tetrad and Boyer-Lindquist coordinates (t,r,θ,ϕ), we assume a time dependence of the form $e^{-i\omega t}$ and a ϕ dependence of the form $e^{im\phi}$, the SWSHs satisfy the equation [4,7]

$$[(1-x^2)\,{}_sS_{\ell m,x}]_{,x} + \left[(cx)^2 - 2csx + s + {}_sA_{\ell m} - \frac{(m+sx)^2}{1-x^2}\right]{}_sS_{\ell m} = 0, \tag{1}$$

where $x \equiv \cos\theta$, $c \equiv a\omega$ and θ is the Boyer-Lindquist polar angle. The angular separation constant ${}_sA_{\ell m}$ is, in general, complex. The spin-weight parameter takes on the values $s = 0, \pm 1/2, \pm 1, \pm 2$ for massless scalar, spinor, vector and tensor perturbations, respectively.

When $s=0$ the SWSHs reduce to the ordinary (scalar) spheroidal wave functions [8]. In the limit $c \to 0$ (corresponding to the Schwarzschild limit) the spin-weighted spheroidal harmonics reduce to spin-weighted spherical harmonics ${}_sY_{\ell m}$ [2,3], for which

$${}_sA_{\ell m} = \ell(\ell+1) - s(s+1) \tag{2}$$

and

$$\int {}_{-2}Y_{\ell m}{}^{*} - 2Y_{\ell' m'} d\Omega = \delta_{\ell,\ell'}\delta_{m,m'}. \tag{3}$$

The ordinary spherical harmonics are spin-weighted spherical harmonics with $s=0$.

The gravitational waves emitted by newly formed Kerr black holes can be decomposed as a superposition of complex quasinormal modes (QNMs) with frequencies $\omega_{\ell mn}$, where the "overtone index" n measures the magnitude of the imaginary part of the frequencies: low-n modes

*eberti@olemiss.edu
†aklein@olemiss.edu

damp most slowly, and therefore they dominate the response of the black hole [9–11]. Each QNM can be associated to a SWSH angular eigenfunction ${}_sS_{\ell mn} \equiv {}_sS_{\ell m}(a\omega_{\ell mn})$ labeled by the corresponding overtone index n [6,7,12]. Due to their importance in black-hole physics, the properties of SWSHs have been investigated in some depth [4,5,13–16]. Press and Teukolsky [5] provided a polynomial fit in c of the eigenvalues ${}_sA_{\ell m}$, which is valid up to $c \sim 3$. A formal perturbation expansion in powers of c was carried out by Fackerell and Crossman [14] (see also [15], where some typos were corrected). Analytic expansions for small and large values of c were discussed and compared to numerical results in [16].

In practice, only the first few QNMs contribute noticeably to the ringdown radiation from a newly formed Kerr black hole. These modes were first investigated in detail by Leaver and Onozawa [7,17]. Higher-order modes may have some relevance in the context of black-hole thermodynamics and quantum gravity (see [18–25]), but they will not be discussed in this paper.

The main motivation for the present study is that the use of spherical harmonics (rather than SWSHs) induces significant *mode mixing* in numerical relativity simulations of black-hole binary mergers. This mixing is particularly evident in the $(\ell = 3, m = 2)$ spin-weighted spherical harmonic mode, where (as first noticed in [26]) the ringdown radiation is a superposition of the ω_{320} and ω_{220} modes. Subsequent studies confirmed this finding [27–31], and it was recently proved beyond any reasonable doubt that the observed QNM mixing occurs because spherical harmonics contain a superposition of several spheroidal harmonics [32–34].

Mathematically, mode mixing occurs because, to leading order in perturbation theory, SWSHs with angular indices (ℓ, m) are a superposition of spherical harmonics with the *same* value of m but different values of $\ell' \neq \ell$. As shown by Press and Teukolsky [5],

$$ {}_sS_{\ell m} = {}_sY_{\ell m} + \sum_{\ell' \neq \ell} \frac{\langle s\ell' m|\mathfrak{h}_1|s\ell m\rangle}{\ell(\ell+1) - \ell'(\ell'+1)} {}_sY_{\ell' m} + \cdots, \quad (4) $$

where the specific form of $\langle s\ell' m|\mathfrak{h}_1|s\ell m\rangle$ is not important for the moment (cf. Appendix for details).

A systematic investigation of the mixing between spherical and spheroidal harmonics is needed to construct semianalytical models of the transition from merger to ringdown, both in the extreme mass-ratio limit [34,35] and for comparable-mass binaries [36,37]. Furthermore, a better understanding of this mixing can help in selecting the optimal frame to analyze generic precessing black-hole binary mergers [38–42]. More in general, a "dictionary" relating spherical and spheroidal modes is useful in all applications of black-hole perturbation theory.

Quite surprisingly (and to the best of our knowledge) no systematic investigation of mode mixing is available in the literature. The main goal of this paper is to fill this gap by computing the complex universal functions $\mu_{m\ell\ell' n'}(j)$ of the dimensionless black-hole spin $j \equiv a/M \in [0, 1]$ defined by the following inner product:

$$ \int {}_sS^*_{\ell' m' n'} {}_sY_{\ell m} d\Omega = \mu_{m\ell\ell' n'}(j)\delta_{m,m'}, \quad (5) $$

where $s = -2$, -1 or 0, and the Kronecker symbol $\delta_{m,m'}$ comes from the $e^{im\phi}$ dependence of the harmonics.

Another goal of this paper is to produce a catalog of the following quantities, that are of interest for ringdown data analysis in the context of gravitational-wave detection [12,43]:

$$ \int {}_sS_{\ell' m' n'}{}^* {}_{-2}S_{\ell mn} d\Omega = \alpha_{m\ell\ell' nn'}(j)\delta_{m,m'}. \quad (6) $$

The functions $\alpha_{m\ell\ell' nn'}(j)$ were evaluated numerically for specific values of the indices and for a single value of the spin parameter ($j = 0.98$ in Table I, and $j = 0.8$ in Tables II and III) in [16]. Here we extend that calculation to all dominant modes and to all values of $j \in [0, 1]$. Our numerical results for both sets of coefficients $\mu_{m\ell\ell' n'}(j)$ (henceforth the *spherical-spheroidal mixing coefficients*) and $\alpha_{m\ell\ell' nn'}(j)$ (henceforth the *spheroidal-spheroidal mixing coefficients*) are available online [44].

In Fig. 1 we illustrate the importance of going beyond the Press-Teukolsky perturbation-theory calculation in computing the mixing coefficients. There we consider the fundamental ($n' = 0$) QNM with $m = 2$ and we plot $\mu_{m\ell\ell' n'}(j)$ for $\ell = 2, 3$, $\ell' = 2, 3$, i.e. for the dominant multipoles in binary black-hole mergers. The plot compares: (1) the numerical calculation of the coefficients $\mu_{2\ell\ell' 0}$ reported in this paper, (2) a power-law fit to the numerical results [cf. Eq. (11) below], and (3) the approximate value of these coefficients predicted by the Press-Teukolsky expansion of Eq. (4). Figure 1 shows that the Press-Teukolsky approximation is adequate for small spins, but it is not accurate enough for fast rotating black holes, with relative errors[1] of order $\sim$30% when $j \to 1$ even for $n' = 0$.

The outline of the paper is as follows. We first recall some properties of the SWSHs (Sec. II). Then we show the results of our numerical calculation of the mixing coefficients and we give analytical fits of the j dependence of the cofficients (Sec. III). In the conclusions we point out

[1] Analyzing the analytical predictions for different $\mu_{m\ell\ell' n'}$ at the maximum spin value considered here of 0.999, we find that (i) the absolute deviations form the analytical prediction in the mixing coefficients for counterrotating modes ($m < 0$) when $\ell = \ell'$ can be of order unity for large n', and are consistently in excess of 0.5 for $n' \geq 3$, and (ii) the relative deviations for $m > 0$ and $\ell \neq \ell'$ are most of the time beyond 10%, e.g. they are between 27% and 29% for $\mu_{223n'}$ irrespective of n'.

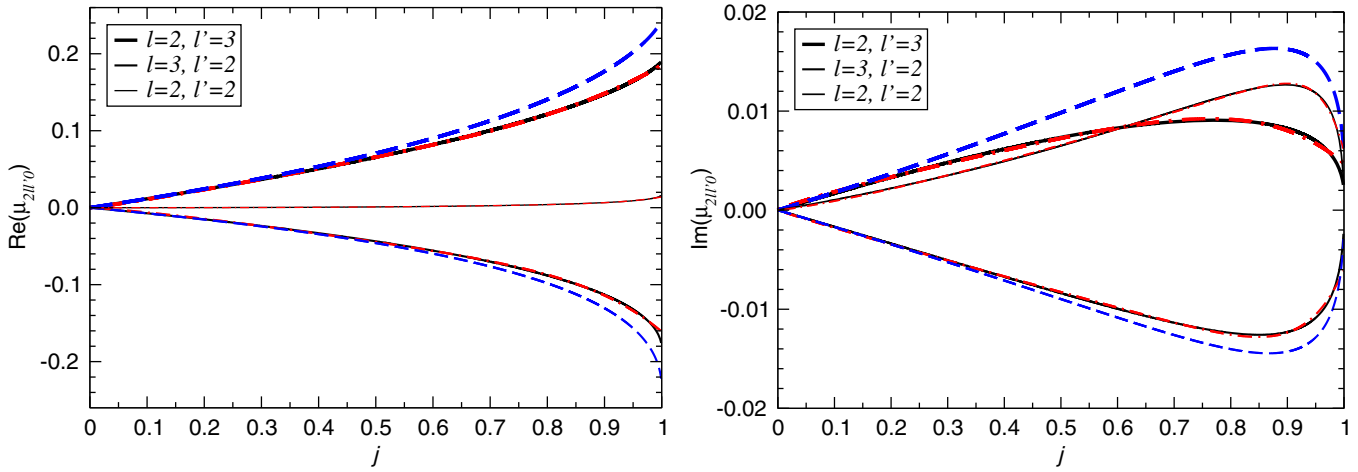

FIG. 1 (color online). Real (left panel) and imaginary part (right panel) of the spherical-spheroidal mixing coefficients $\mu_{m\ell\ell' n'}$ for $m = 2$, $n' = 0$. Here we consider the dominant multipoles ($\ell = 2, \ell' = 3$) (very thick lines in the upper half of each panel), ($\ell = 3, \ell' = 2$) (thick lines in the lower half of each panel) and ($\ell = \ell' = 2$) (thin lines in each panel). Solid lines (black online) correspond to the numerical calculation presented in this paper; dash-dotted lines (red online, almost indistinguishable from the black lines) are the fitting relations of Eq. (11); dashed lines (blue online) are the leading-order Press-Teukolsky approximation [5]. In the case $\ell = \ell' = 2$ the mixing coefficients are close to unity, so we actually plot $1 - \mu_{2220}$; furthermore, to leading order the Press-Teukolsky calculation predicts that they are exactly equal to unity, so their approximation is not shown in the plot.

possible applications of this calculation and directions for future work.

II. SPIN-WEIGHTED SPHEROIDAL HARMONICS

Leaver [7] found the following series solution of the SWSH equation (1):

$$ {}_sS_{\ell mn}(\theta,\phi) = e^{im\phi} e^{c_{\ell mn} x} (1+x)^{k_-} (1-x)^{k_+} \sum_{p=0}^{\infty} a_p (1+x)^p, \tag{7}$$

where $k_\pm \equiv |m \pm s|/2$, and $x = \cos\theta$. The expansion coefficients a_p are obtained from a three-term recursion relation that can be found, e.g., in [7,16].

The angular separation constant ${}_sA_{\ell mn}$, $c_{\ell mn} = a\omega_{\ell mn}$ and the SWSHs ${}_sS_{\ell mn}$ are, in general, complex. They take on real values only in the oblate case ($c_{\ell mn} \in \mathbb{R}$) or, alternatively, in the prolate case ($c_{\ell mn}$ pure imaginary) with $s = 0$. Some useful symmetry properties hold (see eg. [7]):

(i) given eigenvalues for (say) $m > 0$, those for $m < 0$ are readily obtained by complex conjugation:

$$ {}_sA_{\ell mn} = {}_sA^*_{\ell -mn}; \tag{8}$$

(ii) given eigenvalues for (say) $s < 0$, those for $s > 0$ are given by

$$ {}_{-s}A_{\ell mn} = {}_sA_{\ell mn} + 2s. \tag{9}$$

Exploiting these symmetries, in our numerical calculations we only consider $s \leq 0$ and $m \geq 0$. In practice this means that we only compute the positive-frequency QNMs, even though each mode consists of *both* a positive-frequency and a negative-frequency component: see [7,12] for more extensive discussions.

(iii) Let us define $\rho_{\ell mn} \equiv ic_{\ell mn}$. If $\rho_{\ell mn}$ and ${}_{-s}A_{\ell mn}$ correspond to a solution for given (s, l, m, n), then another solution can be obtained by the following replacements: $m \to -m$, $\rho_{\ell mn} \to \rho^*_{\ell mn}$, ${}_{-s}A_{\ell mn} \to {}_{-s}A^*_{\ell -mn}$.

Leaver's solution gives a simple and practical algorithm for the numerical calculation of eigenvalues ${}_sA_{\ell mn}$ and eigenfunctions ${}_sS_{\ell mn}$ for a perturbed Kerr black hole. The procedure we use is standard and it is described in many papers [7,10,17,45], so here we give a very concise summary. Start from the analytically known angular eigenvalue for a given overtone n in the Schwarzschild limit, Eq. (2). In the Kerr space-time, linear gravitational perturbations are described by a pair of coupled differential equations: one for the angular part of the perturbations, and the other for the radial part. The radial equation is given, e.g., in [4,7]. The angular equation is the SWSH equation (1). Boundary conditions for the two equations can be cast as a pair of three-term continued fraction relations. Solve the radial continued-fraction equation to find $\omega_{\ell mn}$ in the Schwarzschild limit. Now increase j in small increments and, for given values of (s, ℓ, m, n), look for simultaneous zeros of the radial and angular continued fraction equations to find both the "radial eigenvalue" $\omega_{\ell mn}$ and the angular separation constant ${}_sA_{\ell mn}$, using the values computed for smaller j as initial guesses in the numerical search. Once the radial and angular eigenvalues are known, the series coefficients a_p can be computed using the

recursion relation and plugged into the series solution (7) to get the corresponding eigenfunction to the required precision. In our numerical calculations we truncate the series at some $p = p_{\max}$ such that the inclusion of subsequent terms would not modify the series by more than one part in 10^6. This algorithm only determines the eigenfunction up to a normalization constant, which can easily be fixed by imposing the normalization condition

$$\int |{}_sS_{\ell mn}|^2 d\Omega = 1. \tag{10}$$

III. MIXING COEFFICIENTS

In this section we present and discuss our numerical results for both, the spherical-spheroidal mixing coefficients $\mu_{m\ell\ell' n'}(j)$ and the spheroidal-spheroidal mixing coefficients $\alpha_{m\ell\ell' nn'}(j)$. We also present power-law fits of the dependence of these coefficients on the dimensionless Kerr parameter j.

A. The spherical-spheroidal mixing coefficients

Figure 2 shows how the mixing coefficients for $\ell = \ell' = 2$ and $m = 2$ (left) or $m = 1$ (right) behave for the first eight QNMs ($n' = 0, \ldots, 7$) as the Kerr parameter increases from the Schwarzschild limit $j = 0$ (where $\mu_{m\ell\ell' n'} = 1$) to the extremal Kerr limit $j = 1$. Each curve can be thought of as a parametric plot, where the parameter along the curve is j. Circles denote the following discrete values of j: $j = 0, 0.1, 0.2, \ldots, 0.9, 0.99$. The numerical data are truncated at $j = 0.999$, because the behavior of QNMs for values of j very close to unity requires a special treatment [46,47].

As first shown by Detweiler, for corotating modes with $\ell = m$ the imaginary part of the quasinormal frequencies goes to zero as $j \to 1$ [48]. The physical reason for this behavior is that QNMs can be thought of as perturbations of null geodesics [46,47,49–51]. In the extremal limit the spherical photon orbit approaches the horizon and the frequency of most QNMs with $\ell = m$ becomes equal to $m\Omega_{\rm H}$, where $\Omega_{\rm H} = a/(2Mr_+)$ is the angular velocity and $r_+ = M + \sqrt{M^2 - a^2}$ is the Boyer-Lindquist radius of the (outer) horizon. Whenever the QNM frequency tends to the critical value for superradiance $m\Omega_{\rm H}$ the black hole becomes marginally unstable, the eigenvalues of the SWSHs become real, and the SWSHs themselves become oblate in the language of Flammer's monograph [8]. A surprising exception to this rule is the overtone with $n' = 5$: this oddity was first noticed by Onozawa (cf. Fig. 4 of [17]). As a consequence, the mixing coefficient corresponding to the mode with $n' = 5$ in the left panel of Fig. 2 is also exceptional, and it does not "turn around" to meet the other modes on the real axis as $j \to 1$.

Figure 3 shows the dominant mixing coefficients for the first eight QNMs ($n' = 0, \ldots, 7$) with $(\ell, \ell') = (2, 3)$, $(\ell, \ell') = (3, 2)$ and $m = 2$ or $m = -2$. We choose to display these particular values of the mixing coefficients because they are the most relevant to explain the spherical-spheroidal mode mixing studied in [32,33] (for the $m = 2$ modes of comparable mass black-hole mergers) and [34] (for the $m = \pm 2$ modes of extreme-mass-ratio black-hole mergers). Once again, note that the inner product becomes purely real near the superradiant frequency for modes with $m = 2$, because the imaginary part of the QNM frequencies with $\ell = m$ tends to zero and the harmonics become oblate—the overtone with $n' = 5$ being, again, the exception. The plot also highlights the fact that the absolute value

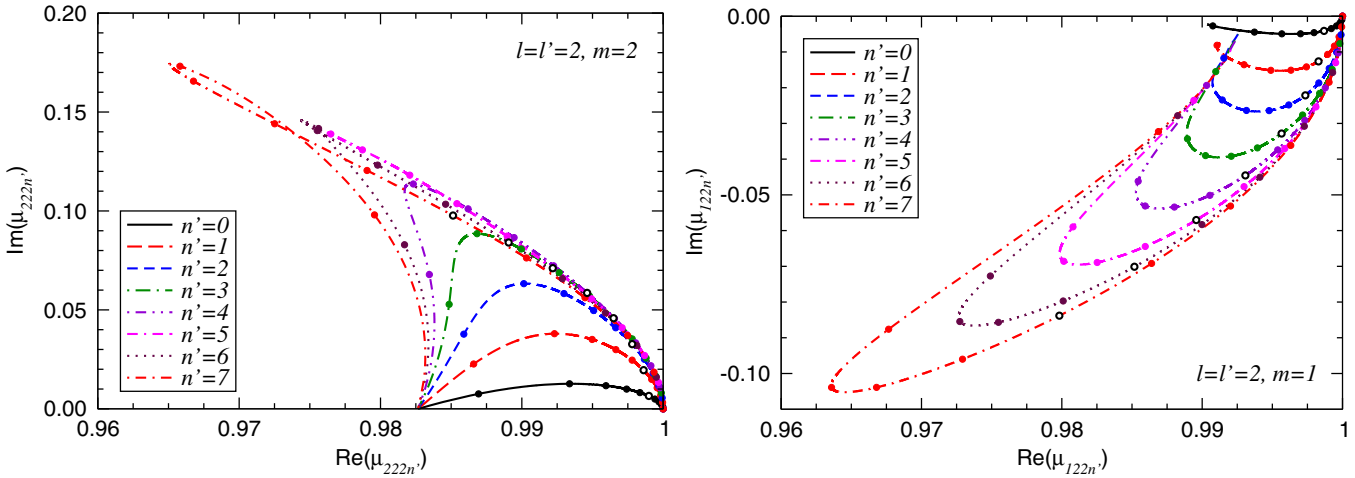

FIG. 2 (color online). Trajectories traced by the mixing coefficients $\mu_{m\ell\ell' n'}$ with $\ell = \ell' = 2$, $m = 2$ (left panel) and $m = 1$ (right panel) as the Kerr parameter increases from $j = 0$ (where $\mu_{m22n'} = 1$) to the nearly extremal Kerr limit. Each curve can be thought of as a parametric plot, where the parameter is j. Filled circles denote the following discrete values of j: $j = 0, 0.1, 0.2, \ldots, 0.9, 0.99$. To guide the eye, along each trajectory the dimensionless Kerr parameter $j = 0.5$ is denoted by a hollow circle.

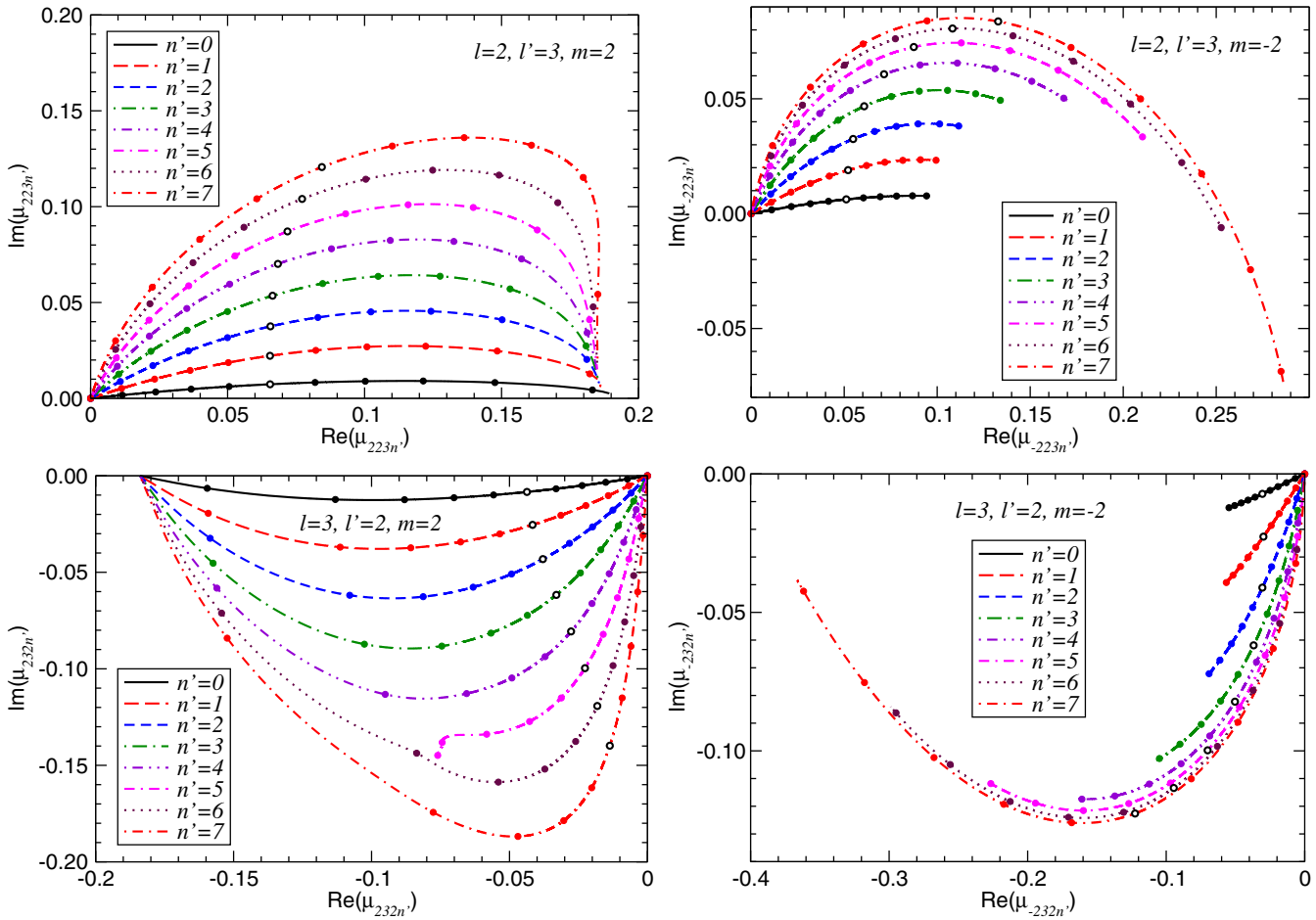

FIG. 3 (color online). Trajectories traced by the mixing coefficients $\mu_{m\ell\ell' n'}$ in the complex plane as the Kerr parameter increases from $j = 0$ (where $\mu_{m\ell\ell' n'} = 0$ for $\ell \neq \ell'$) to $j = 1$. Panels in the top row refer to $(\ell, \ell') = (2, 3)$, those in the bottom row to $(\ell, \ell') = (3, 2)$; left panels are for $m = 2$, right panels for $m = -2$.

of the mixing coefficients is typically larger for large spins (at fixed overtone number n') and for large overtone numbers (at fixed spin j).

In Fig. 4 we plot the absolute value of the mixing coefficients $|\mu_{m\ell\ell' n'}|$ with $\ell = 2$, $m = 2$, $n' = 0$ as ℓ' increases. The figure shows that (perhaps unsurprisingly) mode coupling decays roughly exponentially with $|\ell' - \ell|$.

Numerical tables of $\mu_{m\ell\ell' n'}(j)$ for all modes with $|s| \leq \ell \leq 7$, $-\ell \leq m \leq \ell$, $-\ell' \leq m \leq \ell'$, $0 \leq n' \leq 7$ for $s = -2$, and $0 \leq n' \leq 3$ for $s = -1$ and $s = 0$ can be found online [44].

B. The spheroidal-spheroidal mixing coefficients

Motivated by the fact that ringdown waveforms should be expanded in terms of SWSHs rather than spin-weighted spherical harmonics [12], Ref. [16] carried out a limited and preliminary investigation of the spheroidal-spheroidal mixing coefficients. Table I of [16] compared a numerical calculation of selected spheroidal-spheroidal mixing

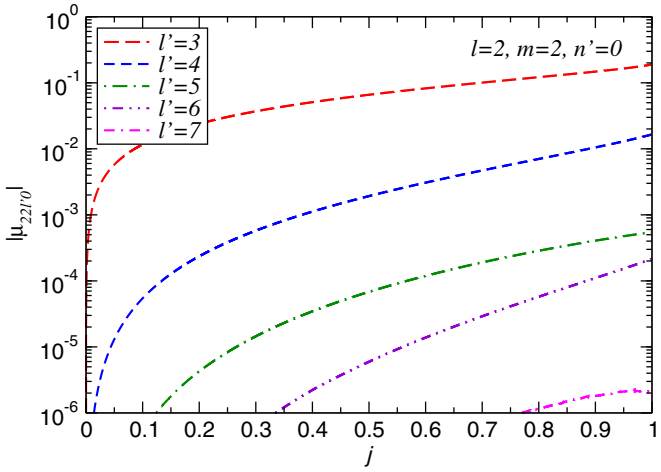

FIG. 4 (color online). Absolute values of the mixing coefficients $|\mu_{m\ell\ell' n'}|$ with $\ell = m = 2$, $n' = 0$ and different values of $\ell' = 3, \ldots, 7$, illustrating the roughly exponential decay of the mixing coefficients with $|\ell' - \ell|$.

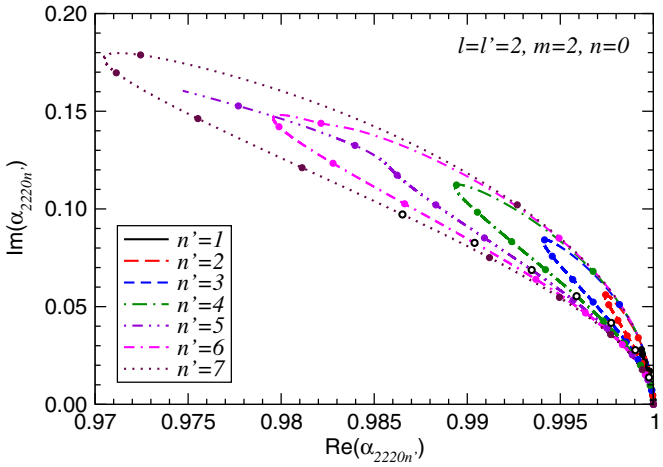

FIG. 5 (color online). Trajectories described in the complex plane by the spheroidal-spheroidal mixing coefficients $\alpha_{m\ell\ell' nn'}(j)$ with $\ell = \ell' = m = 2$, $n = 0$ and different values of the *overtone index* $n' \geq 1$ as the dimensionless spin increases from $j = 0$ to $j = 1$.

coefficients $\alpha_{m\ell\ell' nn'}(j)$, as defined in Eq. (6), with the Press-Teukolsky perturbation theory calculation. The constants $\alpha_{m\ell\ell' nn'}(j)$ computed using Leaver's method were listed in Tables II and III of [16] for $j = 0.8$ and selected values of the indices.

Here we extend those preliminary calculations to generic values of j and to all modes of relevance for gravitational-wave data analysis. Representative results are shown in Figs. 5 and 6. Figure 5 shows the scalar product between the dominant mode in black-hole binary merger simulations ($\ell = \ell' = m = 2$, $n = 0$) and higher overtones with the same angular dependence (same $\ell = \ell' = m$). All modes describe loops that begin and end close to $\alpha_{2220n'} = 1$; the one exception, as usual, is the QNM with $n' = 5$.

The most relevant spheroidal-spheroidal mixing coefficients to understand black-hole binary simulations are small-n overtones with low angular indices (ℓ, ℓ') equal to either 2 or 3. Some of these mixing coefficients are plotted, with the usual conventions, in Fig. 6. In particular, we show (1) the m dependence of spheroidal-spheroidal overlaps when $\ell = 2$, $\ell' = 3$, $n = n' = 0$, and (2) the overlap between the fundamental mode and the first overtone when $\ell = 2$, $\ell' = 3$ and $|m| = 2$.

C. Fitting formulas for the mixing coefficients

As illustrated in Fig. 1, we can reproduce the numerical data for the mixing coefficients to satisfactory accuracy (absolute deviations being typically smaller than 10^{-4} for the dominant modes, and smaller than a few times 10^{-3} for all modes we considered) with the following power-law fits:

$$\begin{aligned} \mathrm{Re}(\mu_{m\ell\ell' n'}) &= \delta_{\ell\ell'} + p_1 j^{p_2} + p_3 j^{p_4}, \\ \mathrm{Im}(\mu_{m\ell\ell' n'}) &= q_1 j^{q_2} + q_3 j^{q_4}. \end{aligned} \tag{11}$$

Table I lists the fitting parameters (p_i, q_i) $(i = 1, \ldots, 4)$ for some combinations of (m, ℓ, ℓ', n') that are particularly relevant in black-hole binary mergers. These values were chosen as particularly significant because

(i) Ref. [33] successfully extracted QNMs with $(\ell, m, n) = (2, 2, 0)$, (3,2,0) and (2,2,1) from numerical simulations of comparable mass black-hole mergers, showing that mode mixing plays an important role in the extraction procedure; and

(ii) Ref. [34] pointed out that mode mixing plays an important role also for extreme mass-ratio binaries (see e.g. their Fig. 7). In addition, they found that negative-m, "counterrotating" modes (or "mirror modes": see [12] for a discussion) contribute to the mixing, because frame dragging can change the

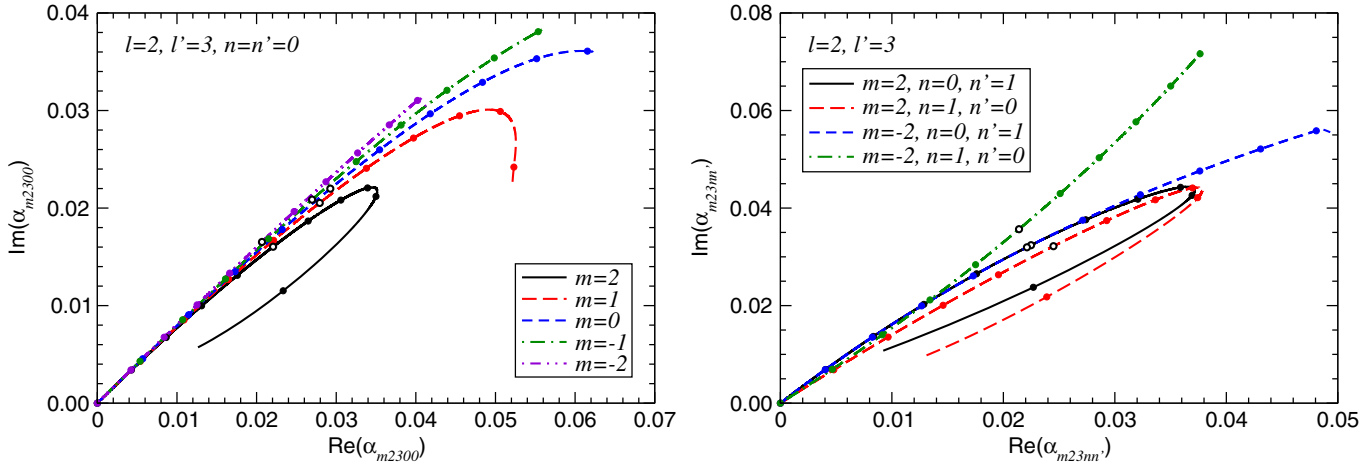

FIG. 6 (color online). Trajectories described in the complex plane by the spheroidal-spheroidal mixing coefficients $\alpha_{m\ell\ell' nn'}(j)$ with: (1) $\ell = 2$, $\ell' = 3$, $n = n' = 0$ and $-\ell \leq m \leq \ell$ (left panel); (2) $\ell = 2$, $\ell' = 3$, $|m| = 2$, and either $(n, n') = (0, 1)$ or $(n, n') = (1, 0)$.

TABLE I. Fitting function parameters in Eq. (11) for some of the $\mu_{m\ell\ell' n'}$'s that are most relevant in black-hole binary modeling.

Indices				$\mathrm{Re}(\mu_{m\ell\ell' n'})$				$\mathrm{Im}(\mu_{m\ell\ell' n'})$			
m	ℓ	ℓ'	n'	$10^5 p_1$	p_2	$10^5 p_3$	p_4	$10^5 q_1$	q_2	$10^5 q_3$	q_4
2	2	2	0	−740	2.889	−661	17.129	1530	1.219	−934	24.992
2	2	2	1	−873	2.655	−539	15.665	4573	1.209	−2801	25.451
2	2	3	0	14095	1.112	4395	6.144	1323	0.854	−852	7.042
2	3	2	0	−10351	1.223	−5750	8.705	−1600	0.953	1003	14.755
−2	2	2	0	−1437	2.118	1035	2.229	−7015	1.005	67	3.527
−2	2	2	1	−2659	2.007	53	4.245	−21809	1.008	221	4.248
−2	2	3	0	14971	1.048	−5463	1.358	18467	1.015	−10753	1.876
−2	3	2	0	−13475	1.088	7963	1.279	−1744	1.011	516	1.821

sign of the orbital frequency of the plunging particle. This finding was confirmed by more recent time-domain calculations [35].

Table I is only representative. Comprehensive tables listing these fitting parameters for scalar, electromagnetic and gravitational modes with $|s| \leq \ell \leq 7$, $-\ell \leq m \leq \ell$, $-\ell \leq m' \leq \ell$, $0 \leq n' \leq 7$, $s = -2$ are publicly available online at [44], where we also provide fitting parameters for the $\alpha_{m\ell\ell' nn'}$'s.

IV. CONCLUSIONS

This paper was mainly motivated by recent investigations of spherical-spheroidal mode mixing in black-hole binary mergers [26,32–34]. For this reason our analysis was limited to four-dimensional SWSHs and low-order overtones. Despite these limitations, we expect the dictionary developed in this paper to be useful in several applications of black hole perturbation theory, including the construction of phenomenological models of black-hole mergers, studies of Green's functions in black-hole backgrounds, self-force investigations (see e.g. [52,53]) and calculations of Hawking radiation.

It would be interesting to extend our work to higher overtones, that may have some relation with black-hole area quantization (see e.g. [18–25]), or [10,45] for reviews). It would also be useful to investigate mixing coefficients for higher-dimensional spheroidal harmonics, that are of interest for the phenomenology of black-hole formation in high-energy particle collisions [54] and to assess the stability of higher-dimensional rotating black holes [16,55–59]. Furthermore our analysis was limited to spin values that are not very close to $j = 1$, and it calls for a more careful investigation of the nearly extremal regime, where a bifurcation of the spectrum can occur [46,47] and lead to turbulent behavior [60].

The numerical data and fitting coefficients computed in this paper are publicly available for download [44]. The webpage includes also spherical-spheroidal mixing coefficients for SWSHs with $s = -1$ and $s = 0$, that were not reported in this paper because they are qualitatively similar to the data for spin weight $s = -2$.

ACKNOWLEDGMENTS

We are grateful to Michalis Agathos, Riccardo Sturani, Scott Hughes, Alessandra Buonanno, Andrea Taracchini, Gaurav Khanna and Sebastiano Bernuzzi for correspondence and conversations that stimulated our interest in this problem. This research was supported by NSF CAREER Grant No. PHY-1055103.

APPENDIX: PERTURBATIVE EVALUATION OF THE MIXING COEFFICIENTS

As mentioned in the main text, the SWSH equation can be solved via an expansion in powers of c using standard perturbation theory [5]. For $c = 0$ the solutions are ordinary spin-weighted spherical harmonics [2,3]. The next-order correction can be found in Eq. (3.7) of Ref. [5] (see also Appendix F of [61]); the result is Eq. (4), where

$$\langle s\ell' m|\mathfrak{h}_1|s\ell m\rangle = \int {}_sY^*_{\ell' m}\mathfrak{h}_{1s}Y_{\ell m}d\Omega, \tag{A1}$$

$$\mathfrak{h}_1 \equiv (a\omega)^2\cos^2\theta - 2a\omega s\cos\theta. \tag{A2}$$

The integral can be evaluated using the identities

$$\langle s\ell' m|\cos\theta|s\ell m\rangle = \left(\frac{2\ell+1}{2\ell'+1}\right)^{1/2}\langle \ell, 1, m, 0|\ell', m\rangle\langle \ell, 1, -s, 0|\ell', -s\rangle,$$

$$\langle s\ell' m|\cos^2\theta|s\ell m\rangle = \frac{1}{3}\delta_{\ell,\ell'} + \frac{2}{3}\left(\frac{2\ell+1}{2\ell'+1}\right)^{1/2}\langle \ell, 2, m, 0|\ell', m\rangle\langle \ell, 2, -s, 0|\ell', -s\rangle,$$

where $\langle \ell_1, \ell_2, m_1, m_2|L, M\rangle$ is a Clebsch-Gordan coefficient.

[1] K. Thorne, Rev. Mod. Phys. **52**, 299 (1980).
[2] E. Newman and R. Penrose, J. Math. Phys. (N.Y.) **7**, 863 (1966).
[3] J. Goldberg, A. MacFarlane, E. Newman, F. Rohrlich, and E. Sudarshan, J. Math. Phys. (N.Y.) **8**, 2155 (1967).
[4] S. A. Teukolsky, Astrophys. J. **185**, 635 (1973).
[5] W. H. Press and S. A. Teukolsky, Astrophys. J. **185**, 649 (1973).
[6] E. W. Leaver, J. Math. Phys. (N.Y.) **27**, 1238 (1986).
[7] E. Leaver, Proc. R. Soc. A **402**, 285 (1985).
[8] C. Flammer, *Spheroidal Wave Functions* (Stanford University Press, Stanford, CA, 1957).
[9] K. D. Kokkotas and B. G. Schmidt, Living Rev. Relativity **2**, 2 (1999).
[10] E. Berti, V. Cardoso, and A. O. Starinets, Classical Quantum Gravity **26**, 163001 (2009).
[11] R. Konoplya and A. Zhidenko, Rev. Mod. Phys. **83**, 793 (2011).
[12] E. Berti, V. Cardoso, and C. M. Will, Phys. Rev. D **73**, 064030 (2006).
[13] R. A. Breuer, *Gravitational Perturbation Theory and Synchrotron Radiation*, Lecture Notes in Physics Vol. 44 (Springer-Verlag, New York, 1975).
[14] E. D. Fackerell and R. G. Crossman, J. Math. Phys. (N.Y.) **18**, 1849 (1977).
[15] E. Seidel, Classical Quantum Gravity **6**, 1057 (1989).
[16] E. Berti, V. Cardoso, and M. Casals, Phys. Rev. D **73**, 024013 (2006).
[17] H. Onozawa, Phys. Rev. D **55**, 3593 (1997).
[18] E. Berti and K. D. Kokkotas, Phys. Rev. D **68**, 044027 (2003).
[19] E. Berti, V. Cardoso, K. D. Kokkotas, and H. Onozawa, Phys. Rev. D **68**, 124018 (2003).
[20] A. Neitzke, arXiv:hep-th/0304080.
[21] E. Berti, V. Cardoso, and S. Yoshida, Phys. Rev. D **69**, 124018 (2004).
[22] S. Hod and U. Keshet, Classical Quantum Gravity **22**, L71 (2005).
[23] U. Keshet and S. Hod, Phys. Rev. D **76**, 061501 (2007).
[24] U. Keshet and A. Neitzke, Phys. Rev. D **78**, 044006 (2008).
[25] H.-c. Kao and D. Tomino, Phys. Rev. D **77**, 127503 (2008).
[26] A. Buonanno, G. B. Cook, and F. Pretorius, Phys. Rev. D **75**, 124018 (2007).
[27] E. Berti, V. Cardoso, J. Gonzalez, U. Sperhake, M. Hannam, S. Husa, and B. Brügmann, Phys. Rev. D **76**, 064034 (2007).
[28] J. D. Schnittman, A. Buonanno, J. R. van Meter, J. G. Baker, W. D. Boggs, J. Centrella, B. J. Kelly, and S. T. McWilliams, Phys. Rev. D **77**, 044031 (2008).
[29] J. G. Baker, W. D. Boggs, J. Centrella, B. J. Kelly, S. T. McWilliams, and J. R. van Meter, Phys. Rev. D **78**, 044046 (2008).
[30] B. J. Kelly, J. G. Baker, W. D. Boggs, S. T. McWilliams, and J. Centrella, Phys. Rev. D **84**, 084009 (2011).
[31] Y. Pan, A. Buonanno, M. Boyle, L. T. Buchman, L. E. Kidder, H. P. Pfeiffer, and M. A. Scheel, Phys. Rev. D **84**, 124052 (2011).
[32] B. J. Kelly and J. G. Baker, Phys. Rev. D **87**, 084004 (2013).
[33] L. London, J. Healy, and D. Shoemaker, arXiv:1404.3197.
[34] A. Taracchini, A. Buonanno, G. Khanna, and S. A. Hughes, Phys. Rev. D **90**, DR11250 (2014).
[35] E. Harms, S. Bernuzzi, A. Nagar, and A. Zenginoglu, arXiv:1406.5983.
[36] T. Damour and A. Nagar, arXiv:1406.0401.
[37] J. Healy, P. Laguna, and D. Shoemaker, arXiv:1407.5989.
[38] L. Gualtieri, E. Berti, V. Cardoso, and U. Sperhake, Phys. Rev. D **78**, 044024 (2008).
[39] M. Campanelli, C. O. Lousto, H. Nakano, and Y. Zlochower, Phys. Rev. D **79**, 084010 (2009).
[40] R. O'Shaughnessy, B. Vaishnav, J. Healy, Z. Meeks, and D. Shoemaker, Phys. Rev. D **84**, 124002 (2011).
[41] M. Boyle, R. Owen, and H. P. Pfeiffer, Phys. Rev. D **84**, 124011 (2011).
[42] M. Boyle, Phys. Rev. D **87**, 104006 (2013).
[43] E. Berti, J. Cardoso, V. Cardoso, and M. Cavaglia, Phys. Rev. D **76**, 104044 (2007).
[44] Webpage with MATHEMATICA notebooks and numerical quasinormal mode tables: http://www.phy.olemiss.edu/~berti/qnms.html.
[45] E. Berti, *Conf. Proc.*, C0405132 (2004) 145 [arXiv:gr-qc/0411025].
[46] H. Yang, F. Zhang, A. Zimmerman, D. Nichols, E. Berti, and Y. Chen, Phys. Rev. D **87**, 041502 (2013).
[47] H. Yang, A. Zimmerman, A. Zenginolu, F. Zhang, E. Berti, and Y. Chen, Phys. Rev. D **88**, 044047 (2013).
[48] S. L. Detweiler, Astrophys. J. **239**, 292 (1980).
[49] B. Mashhoon, Phys. Rev. D **31**, 290 (1985).
[50] V. Cardoso, A. S. Miranda, E. Berti, H. Witek, and V. T. Zanchin, Phys. Rev. D **79**, 064016 (2009).
[51] H. Yang, D. A. Nichols, F. Zhang, A. Zimmerman, Z. Zhang, and Y. Chen, Phys. Rev. D **86**, 104006 (2012).
[52] M. Casals, S. Dolan, A. C. Ottewill, and B. Wardell, Phys. Rev. D **88**, 044022 (2013).
[53] B. Wardell, C. R. Galley, A. Zenginoglu, M. Casals, S. R. Dolan, and A. C. Ottewill, Phys. Rev. D **89**, 084021 (2014).
[54] P. Kanti, Int. J. Mod. Phys. A **19**, 4899 (2004).
[55] V. P. Frolov and D. Stojkovic, Phys. Rev. D **67**, 084004 (2003).
[56] D. Ida, Y. Uchida, and Y. Morisawa, Phys. Rev. D **67**, 084019 (2003).
[57] H. K. Kunduri, J. Lucietti, and H. S. Reall, Phys. Rev. D **74**, 084021 (2006).
[58] P. Hoxha, R. Martinez-Acosta, and C. Pope, Classical Quantum Gravity **17**, 4207 (2000).
[59] O. J. Dias, G. T. Horowitz, D. Marolf, and J. E. Santos, Classical Quantum Gravity **29**, 235019 (2012).
[60] H. Yang, A. Zimmerman, and L. Lehner, arXiv:1402.4859.
[61] H. Tagoshi, M. Shibata, T. Tanaka, and M. Sasaki, Phys. Rev. D **54**, 1439 (1996).